Energy 221 (2021) 119893

Contents lists available at ScienceDirect

Energy

journal homepage: www.elsevier.com/locate/energy

Considerations on factors affecting biochar densification behavior based on a multiparameter model

Lorenzo Riva [a, *], Liang Wang [b], Giulia Ravenni [c], Pietro Bartocci [d], Therese Videm Buø [e], Øyvind Skreiberg [b], Francesco Fantozzi [d], Henrik Kofoed Nielsen [a]

[a] Department of Engineering Sciences, University of Agder, Postboks 509, 4898, Grimstad, Norway
[b] SINTEF Energy Research, Postboks 4761, Torgarden, Trondheim, Norway
[c] Department of Chemical and Biochemical Engineering, Technical University of Denmark, Frederiksborgvej 399, 4000, Roskilde, Denmark
[d] Department of Engineering, University of Perugia, Via G. Duranti 67, 06125, Perugia, Italy
[e] Elkem Technology, Fiskåveien 10, 4621, Kristiansand, Norway

ARTICLE INFO

Article history:
Received 4 February 2020
Received in revised form
21 December 2020
Accepted 12 January 2021
Available online 19 January 2021

Keywords:
Densification
Pelletization
Modeling
Pyrolysis
Pyrolysis oil
Biochar

ABSTRACT

The optimization of upscaled biochar pelleting is limited by lack of knowledge regarding the effects of process parameters. A multiparameter model, coupled to a single pellet press unit, was for the first time applied to biochar production to predict the upscaled biochar pelleting process behavior. The model permits to estimate in a time and cost-effective way how the die friction forces, quantified through the pellet exiting pressure, are affected by the key process parameters. It was observed that to achieve acceptably low exiting pressures (in the order of 100 MPa), it was critical to produce biochar at high temperatures (e.g. 600 °C). Addition of water as a binder is also beneficial, while pelletization temperature does not significantly affect the exiting pressure. Furthermore, when pyrolysis oil was used as a binder, lower exiting pressures were measured. Biochar returned higher exiting pressure values compared with untreated wood, but lower compared with torrefied wood. Moreover, the correlation between density and compressive strength was also examined. It was found that the exiting pressure trend is a good indicator to estimate the mechanical quality of the pellets.

1. Introduction

With the necessity of abandoning the consumption of fossil fuels, biomass has been targeted as possible substitute. In particular, biochar produced from biomass is very versatile and can be used for many applications. Biochar is a promising alternative of fossil fuels to be used as energy source in heat and power plants [1–4] and reducing agent in metallurgical applications [5–7]. Biochar can also be used as enhancer to improve soil quality [8–10] and as filter in water treatments [11,12], Recently, The Intergovernmental Panel on Climate Change (IPCC) included this material as a carbon neutral option to tackle climate change, recognizing the possibility to contribute as carbon negative source as well [13]. A more comprehensive lists of different uses has been provided in Refs. [14–16].

Among several challenges that are related to the utilization of biochar, the low mechanical strength of biochar, which may lead to considerable mass losses (and therefore increases of costs) in the handling and transportation steps, can be improved by densification [17]. Densification of biochar has been attempted and studied in recent works [17–23], targeting several potential applications in which the use of this material is hindered by -poor mechanical properties. These works focused on the effects of binders on the mechanical properties, combustion properties and co-densification of biochar with untreated biomass or coal. Only a few studies investigated the feasibility of the biochar pelletization process and the properties of the pelletized biochar, focusing on the effects of the pyrolysis temperature on the biochar densification behavior [18,20,21]. With the aim to perform biochar pelletization at industrial scale, it is necessary to assess the feasibility of the process and to quantify the factors affecting the densification of biochar. One important step in that direction might be done by establishing, developing and validating a versatile model that can predict and evaluate the densification behavior of specific biochars. Utilization of such a model could be time and cost efficiently to predict and

* Corresponding author.
E-mail address: lorenzoriva1@outlook.com (L. Riva).

https://doi.org/10.1016/j.energy.2021.119893

Abbreviations

BET	Brunauer-Emmett-Teller
D	density
db	dry basis
IPCC	Intergovernmental Panel on Climate Change
PB	pine biochar
QSDFT	Quenched Solid Density Functional Theory
SEM	scanning electron microscope
TP	torrefied pine
TCD	thermal conductivity detector
TS	tensile strength, UP: untreated pine, wb: wet basis

screen feasibility to pelletize different biochar - binder mixtures in an industrial process. Experimental work in combination with pellet production models has been reported in previous studies to gain a deeper understanding of biomass pelletization and the effects of specific parameters. In particular, Holm et al. [24] used a laboratory scale single pellet press to simulate the densification of biomass in industrial-scale pelletizers. A multiparameter model describing the forces built up along the dies of the pellet mill matrix was consequently developed and validated [24]. The main quality of this model is that it provides a wide set of information of the pelleting behavior of the studied biomasses upon changes in key parameters (e.g. pelleting temperature or water content) by performing a limited number of lab tests. The model was used and validated for evaluating densification of different woody biomasses [25] and further improved and simplified by the same research group [26]. The main assumption of this model is that the densification of the biomass to pellets is possible due to the combination of the roller pressure and the back pressure that is generated by the friction between the material and the walls of the channels [26]. A schematic drawing of the pellet densification process is presented in Fig. 1. This representation mainly focuses on the forces acting along the channel, which can be related to the energy consumed in the pelleting phase and to the stress borne by the channel itself [24]. The pelleting pressure P_x, is the parameter directly associated to the forces acting along the die and therefore it is critical to assess the feasibility of a pelletization process. Moreover, by its definition, a minimization of the pelleting pressure is directly related to a reduction of the overall energy consumption required in the pelleting phase [24]. The investigation of the variation of this factor with the main pelleting parameters can hence provide essential information regarding the feasibility of the process. In the model, P_x is computed in relation to the dimensions of the pellets so to ease any upscaling evaluation. The model however was validated and applied only with woody biomass. More recently, Arnavat et al. demonstrated that it could be successfully used for assessing pelletization of torrefied wood [27]. However, as reported in Refs. [28,29], torrefied wood and biochar differ considerably in terms of physico-chemical properties and it is indeed not obvious to expect biochar to have the same pelleting behavior as torrefied wood. It becomes hence interesting to further study the possibility of using the model for pelletization of biochar and to assess the effects of the biochar pelletization behaviors under different conditions. The application of this model and the results assessment can be a quick and efficient measure which can provide necessary information for the design and operation of industrial scale biochar pelletization, with a potential reduction of time, operational costs, numbers of trial tests and materials needed.

In the present work, pine wood was used as feedstock for biochar production under different pyrolysis temperatures. The multiparameter model was applied to evaluated effects of three parameters, including pyrolysis temperature, added water content and pelletizing pressure, on pelletization behaviors of pine wood biochar. The model was first applied for a base case at fixed pyrolysis temperature, water content and pelleting temperature. Subsequently, the effect of each of these parameters on the biochar pelleting behaviors was evaluated by varying one of them while keeping the other two constants. The model was also applied for studying pelletization of biochar using pyrolysis oil as binder. The use of pyrolysis oil as binder has been investigated in a previous work and resulted a promising measure to improve the quality of biochar pellets [21]. Moreover, pyrolysis oil is a by-product of biochar production, therefore its utilization as pellet binder can be beneficial to optimize the whole biochar value chain, as schematized in Fig. 2.

In previous works, pelletization of wood and torrefaction of wood have been reported [30,31], and the model has been successfully applied to predict pelletization behaviors of these materials. By the knowledge of the authors, the present work is the first to apply the presented multiparameter model to investigate biochar pelletization behavior as well as the effects of some of the most relevant factors on the exiting pressure, in connection to the mechanical properties, aiming at the optimization of the process. Moreover, for the first time, this model is used to assess the inclusion of pyrolysis oil as binder to pelletize biochar and to compare biochar, untreated wood and torrefied wood pelletization. Results from the current work contribute to more detailed understandings about pelletization of different biochar under various conditions. It is critical to upgrade properties of biochar for meeting requirements from different end user applications.

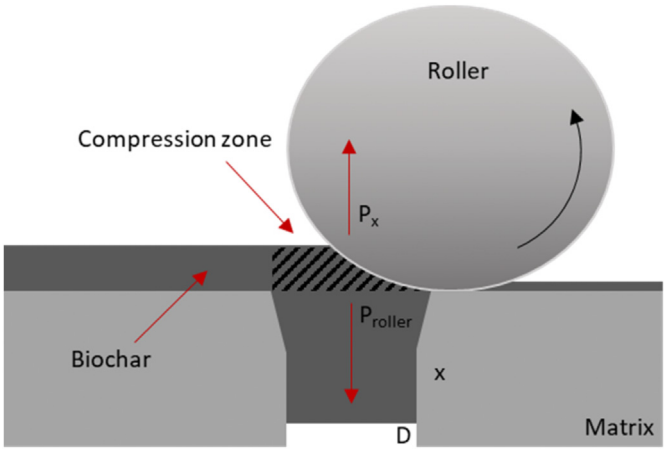

Fig. 1. Pelleting process principle with rotating roller and fixed matrix. D and x are respectively the diameter and the length of the die. P_{roller} is the pressure generated by the roller on the pelletized biomass, while P_x is the pelleting pressure.

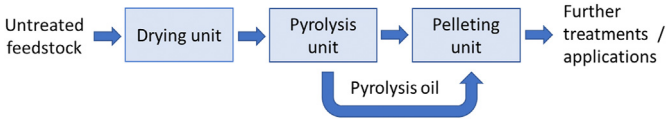

Fig. 2. Conceptual scheme of an integrated pyrolysis-pelletization process, with recovered pyrolysis oil as binder.

2. Material and methods

2.1. Feedstock and biochar production

A Scots Pine (*Pinus Sylvestris*) tree was harvested from a local forest located in Grimstad, Norway. The harvested tree was shredded into chips that were dried at 60 °C for 24 h and stored in an airtight box at ambient temperature. Biochar was produced from the chips at three different pyrolysis temperatures: 400, 600 and 800 °C. A layout of the pyrolysis process is illustrated in Fig. 3. Approximately 100 g of biomass was placed inside the furnace, evenly spread in a silicon carbide retort. The reactor was purged with a flow of 40 ml/min of N_2 to generate inert atmosphere in the reactor. The feedstock was then heated up at a selected rate of 10 °C/min to a desired temperature and kept at that temperature for 1 h. During one experiment, volatiles and gases leaving the reactor were cooled down by two serially connected heat exchangers. The condensable volatiles were collected in a glass bottle. Incondensable gases were not analyzed and were directly expelled through ventilation. After holding at desired temperature for 1 h, heating of the furnace was turned off and the produced biochar was cooled down to room temperature in nitrogen atmosphere to avoid oxidation of the produced biochar. Afterwards, the biochar was unloaded from the reactor and milled in a hammer mill *px-mfc 90 d* (Polymix, Germany) with a 2 mm sieve. The ground biochar produced under different conditions was stored at ambient temperature in airtight boxes. The particle size distribution of the produced biochar was analyzed by a laser diffraction particle size analyzer *Mastersizer 3000* (Malvern, UK). Following the considerations already mentioned in Ref. [20], no further size screening was carried out and pelletization was done with a mixed particle size biochar mixture. The condensates collected from the biochar production experiments were stored in airtight containers at 4 °C, without any further treatment.

2.2. Model theory

The main assumption of this model is that, once the biomass is compressed in one direction, it tends to expand in the two other perpendicular directions. It is therefore possible to relate the pelletizing pressure (P_x), which is equal the pressure the material experiences to exit the die (it will also be referred as exiting pressure), to the Poisson effect by the Poisson's ratio (ν). This ratio ν describes the expansion in directions perpendicular to the direction of compression and under the assumption of orthotropicity, i.e. the biomass fibers are perpendicularly oriented to the longitudinal direction of the channel [27]. The other parameters included in the model are: the pre-stressing term (P_{N0}), incorporating inelasticity, the sliding friction coefficient (μ) and the compression ratio (c). The compression ratio is:

$$c = x/2r \quad \text{Eq.1}$$

where x is the length of the channel and r its radius. By the model presented in Ref. [24], it is then possible to gather all the parameters into the equation for P_x as function of c:

$$P_x(c) = P_{N0}/\nu_{lr}(e^{\mu\nu_{lr}c} - 1) \quad \text{Eq.2}$$

In the Poisson's ratio ν_{lr}, the subscript l denotes the direction of the applied stress (longitudinal) while r denotes the direction of the transverse deformation [25]. Despite its relative simplicity, Eq. 2 has several parameters that need to be derived experimentally, making the model complicated to fit to various biomass whose properties are unknown. In Ref. [26], a new version of Eq. 2 was suggested. It was shown that it is indeed possible to recombine the parameters μ, ν and P_{N0} into two new terms: U and J. Despite these new parameters do not have a direct physical meaning, their definition facilitates the computation of the pelleting curve, or the relation between the compression ratio in the single pellet press and the exiting pressure, by reducing the number of required parameters. Moreover, they can be estimated by a limited number of experiments. Following [26], they are expressed as:

$$U = \mu P_{N0} \quad \text{Eq.3}$$

$$J = \mu\nu_{lr} \quad \text{Eq.4}$$

Inserting Eq. 3 and Eq. 4 into Eq. 2, a simplified version is obtained:

$$P_x(c) = U/J(e^{4Jc} - 1) \quad \text{Eq.5}$$

This new equation, as shown in Ref. [24], for $c \ll 1$ can be reduced to:

$$P_x(c) = 4Uc \quad \text{Eq.6}$$

In Eq. 6, U can therefore be derived experimentally by measuring the exiting pressure (with the method shown in Fig. 4) for pellets made with very low c, by linear fitting. Once U is known, it can be used in Eq. 5 to obtain J. New measurements must be performed at higher c and J can then be extrapolated by non-linear interpolation. It is thus possible with relatively few experiments to obtain all the needed parameters of Eq. 5, and the equation can finally be used. As stated in Ref. [26], the procedure relies on the assumption that the Poisson's ratios are constant with the variation of compression ratios and it is therefore only valid under the assumption that the measurements are made at sufficiently small compression ratios. Moreover, a certain degree of uncertainty is related to the extrapolation of compression ratios that better fit the industrial cases (c = 7–8) [27]. However, the model has been demonstrated to work successfully for wood and torrefied wood [26,27]. The benefits of this model are relevant since:

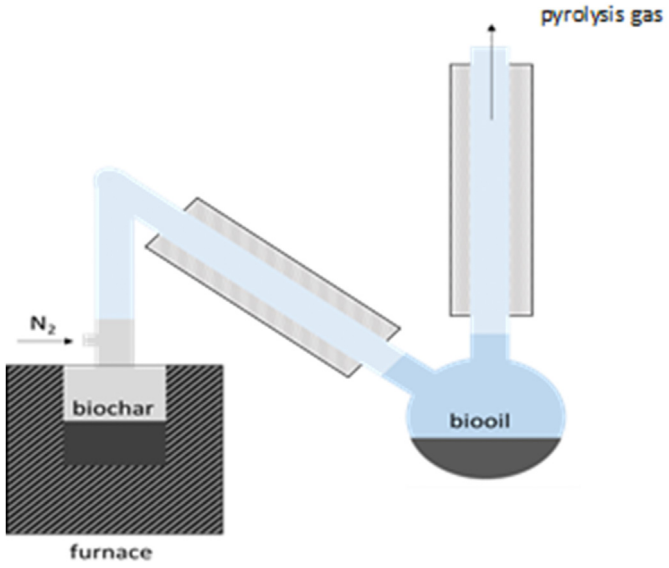

Fig. 3. Layout of the pyrolysis unit with an electrical external heated pyrolysis retort, cooling jackets and collection of pyrolysis oil.

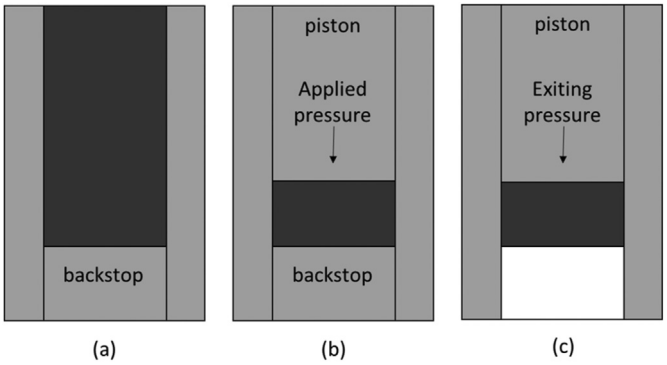

Fig. 4. Lab-scale experiment divided in phases. In phase (a), the backstop is included, and biochar is inserted into to die. In phase (b), the piston compresses the biochar up to a defined pressure. In phase (c), the backstop is excluded, and the pressure necessary to eject the pellet is measured.

- the possibility of building up the curve with a limited number of experiments and material makes it time and material saving;
- limiting the curve parameters to U and J, it becomes easier to understand how external parameters such as pelleting temperature, water content and variations in pelleting material impact on the $P_x(c)$ vs. c curve.

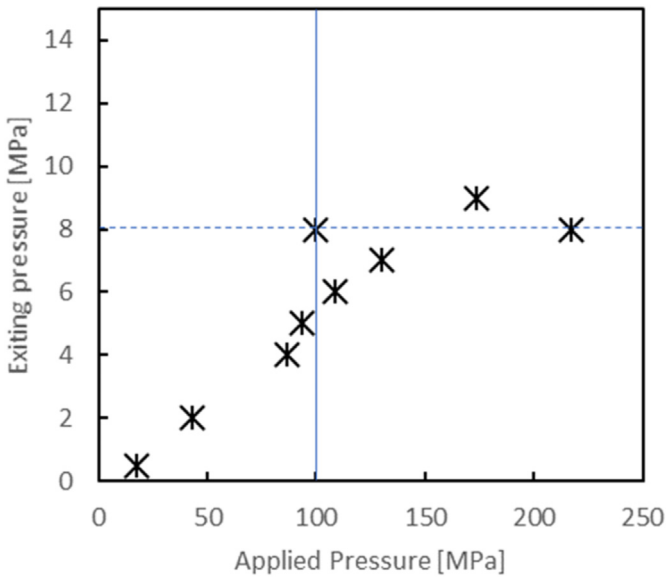

Fig. 5. Measured exiting pressure as function of tested applied pressure for pellets made at 20 °C with biochar produced at 600 °C and a mixing of 35 wt% water. The continuous blue line marks the applied pressure at 100 MPa, while the dotted blue line marks the exiting pressure related to that applied pressure. (For interpretation of the references to colour in this figure legend, the reader is referred to the Web version of this article.)

2.3. Biochar pelletization

For each tested composition, 20 g mixture of biochar and water was prepared at different mass ratios. The considered water contents were 25, 35 and 45%. In accordance with [21], the blending ratios of water and biochar were selected based on results of preliminary studies as it provided an acceptable pellet quality. It was instead observed that at water content values outside the boundaries this was not guaranteed. The blend was homogenized in a beaker by a magnetic stirrer for about 10 min. The biochar with and without mixing of water or binder were pressed by a hot single pellet press (MTI, USA). The inner diameter of the die was 6.25 mm. For press test, the exiting pressure was measured at three different compression ratios below 0.75, so to extrapolate U in the linear region. The diagram point (0, 0) was also included. Each exiting pressure value used to build the pelleting curve was obtained by averaging the results from three different samples at fixed compression ratio. The standard deviation was also computed. The linear interpolation as well as the related equation and R^2 were calculated with Excel. Using the value of the obtained coefficient U and adding three other values/points at higher compression ratios, it was possible to complete the curve by non-linear fitting. This was done in Excel by deriving the coefficient J through the non-linear least squares method. The R^2 of the pelleting curve was obtained by linearization of the exponential curve through logarithmic transformation. In all the experiments, the applied pressure was 100 MPa. This value was chosen because the exiting pressure tends to oscillate around a constant value when the applied pressure was higher than 100 MPa, as can be seen in Fig. 5.

Before pelletization, the die and other moving parts of the single pellet press were heated up to the operating temperature, which was then maintained during the pelletization process. The considered pelleting temperatures were 20, 60, 90 and 120 °C. Pressure was set manually to 100 MPa with a hydraulic piston and kept for 10 s before pressure release and extraction of the pellet. The exiting pressure was measured by a load cell *CPX1000* (Dini Argeo, Italy) connected to a multifunction weight indicator *DFWLB* (Dini Argeo, Italy). Biochar pellets were made by sequential layers pressed at the same pressure when the material was exceeding 0.15 g, according to Ref. [26]. After the process, the pellets were cooled down and stored in airtight boxes at ambient temperature. The list of the configurations that have been tested in this work is presented in Table 1.

2.4. Compressive strength test

The compressive strength of the produced biochar pellets were tested by a pellet hardness tester (Amandus Kahl, Germany). Strength was applied perpendicularly to the cylindrical axis direction. The measured value for compressive strength is normally and here referred to as a tensile strength (TS). Following the procedure in Ref. [32], the tensile strength was computed by the equation:

$$TS = m_s g / \pi r l \qquad \text{Eq.7}$$

where m_s is the force equivalent mass which the pellet hardness tester measures for the obtained strength, g is the gravitational acceleration, r and l respectively are the radius and length of the pellets.

2.5. Pellet density test

The particle density of the biochar pellets was computed indirectly as $\rho = m/\pi r2l$, where m was the mass. Mass was determined on a balance with a readability of 0.1 mg, while radius and length were measured with a Vernier caliper with a precision of 0.01 mm. All density and strength measurements were taken at least 24 h after the pelletization. As shown in Fig. 6, density and compressive strength tend to stabilize when the compression ratio is higher than circa 0.85, for pellets with biochar produced at different pyrolysis temperatures and with water as binder (35% of total weight). For both compressive strength and density measurements, at least

Table 1
List of the configurations that have been tested. Number 1 is referred to also as "base case".

Number	Pyrolysis temperature [°C]	Pelleting temperature [°C]	Water content [wb %]
1	600	20	35
2	600	20	25
3	600	20	45
4	600	60	35
5	600	90	35
6	600	120	35
7	400	20	35
8	800	20	35

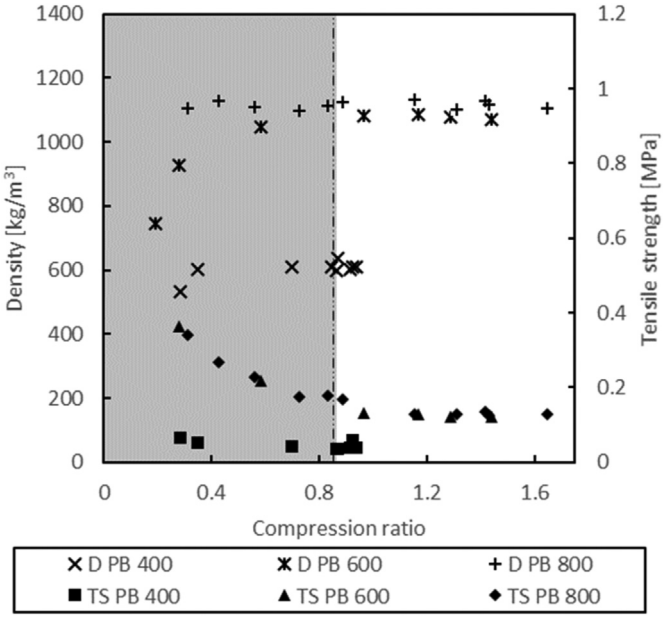

Fig. 6. Density (D) and tensile strength (TS) measured at different compression ratio for pellets of pine biochar (PB) produced at 400, 600 and 800 °C (reported in the legend as 400, 600 and 800) and a water content of 35%. The white region of the area, starting after c = 0.85, highlights the stable zone.

six samples with a compression ratio higher than 0.85 were selected, to avoid the uncertainty region.

2.6. Characterization of pellets and biochar

An *EuroEA* (Eurovector, Italy) with TCD detector was used for the C–H–N ultimate analysis. Oxygen was computed by difference of the other elements. The proximate analysis of the produced biochar was conducted through the procedures described in standards EN 15148, EN 14774–2 and EN 14775, which were applied respectively for volatile matter, moisture content and ash content. Surface area and porosity of the produced biochar were measured with N_2 adsorption at 77 K (*NovaTouch*, Quantachrome, USA). The Brunauer-Emmett-Teller (BET) model was used to calculate the surface area. Pore volume was evaluated with Quenched Solid Density Functional Theory (QSDFT) using the calculation model for slits and cylindrical pores on the adsorption branch. Before each measurement of surface area and porosity, samples were degassed at 150 °C for 10 h. Morphology and microstructure of selected biochar pellet samples were examined by a scanning electron microscopy (Zeiss Ultra 55 limited edition). One biochar pellet was fixed on a sample tap and the outmost surface was scanned.

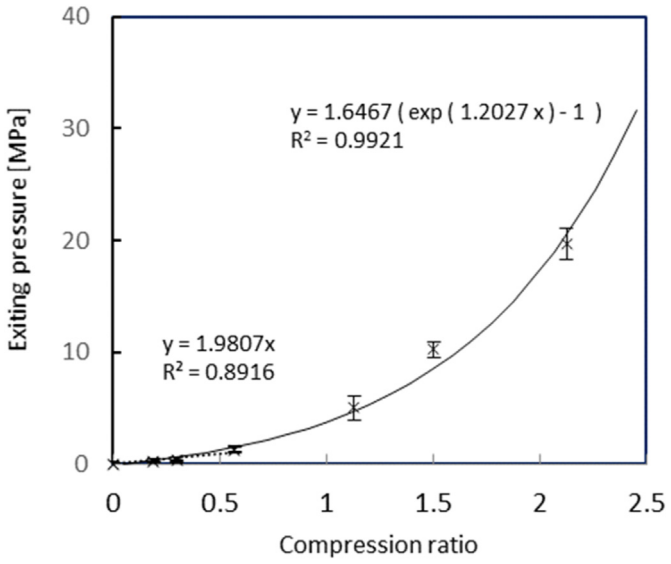

Fig. 7. Experimental data and data fittings to determine the U and J for pellets with biochar produced at 600 °C, pelletized at 25 °C of and with a water content of 35% in the pelletized mixture. The experimental data, displayed with a cross, are the average of the measurements carried at each compression ratio, while the error bars indicate the standard deviations. The dotted line represents the linear region, while the continuous line is the non-linear fitting.

3. Results and discussions

3.1. Determination of the parameters

The model was first applied with biochar produced at 600 °C, mixed with pure water (35% of total weight) and pelletized at 20 °C. In this work, this configuration is also referred to as "base case". The pelleting curve that was obtained is presented in Fig. 7. The first four points (including the diagram point (0, 0)) were used to obtain U by linear fitting. The fitting line is plotted and its equation and R^2 presented right above the curve. The pelleting curve equation is also displayed in Fig. 7. For this configuration U was 0.49 and J was 0.30. The high value of regression coefficient R^2 shows that the model fits well the values from the samples. Small standard deviations show a good repeatability. Generally, the curve shows a similar trend compared to what was observed in Refs. [26,27]. This result shows that the model can successfully be applied for biochar pellets.

3.2. Influence of water as binder

The pelleting curves and the coefficient values for biochar pellets produced with different water contents are presented in Fig. 8 and Fig. 9, respectively. Despite a similar trend in the linear region with compression ratio in the range of 0–1, the curves start deviating more evidently towards the fully exponential zone. It can be noticed that, at fixed compression ratio, a higher water content is tendentially related to a lower exiting pressure. It can also be observed that both U and J tend to decrease with increasing water content. However, the degree of uncertainty makes it difficult to attempt any more precise correlation between these coefficients and the water content.

The beneficial effect of water on reducing exiting pressure of a biomass single pellet press has been reported in Refs. [33,34]. As stated in Ref. [34], pelletization of biomass is generally strongly affected by addition of water. Densification consists of the mechanical interlocking of fibers either by adhesion forces between

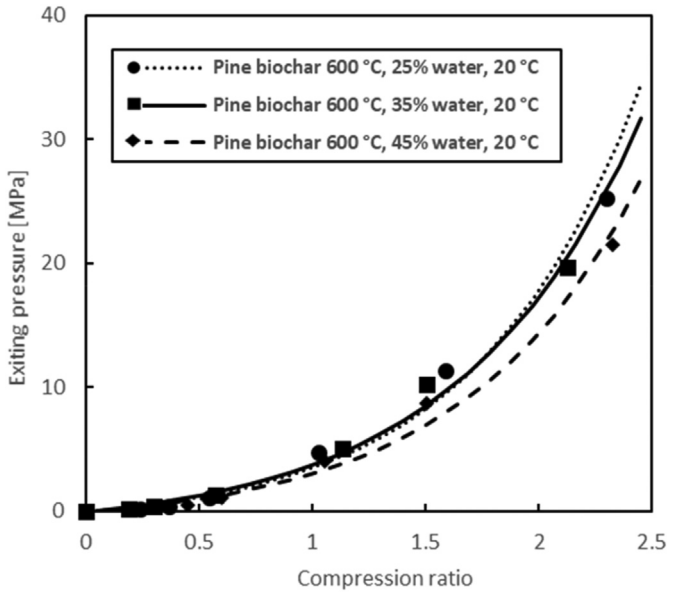

Fig. 8. Exiting pressure curves for biochar produced at 600 °C and pelletized at 20 °C with different water contents. For each configuration, the legend shows a marker and a line. The markers display the experimental data, while the three line represents the modeled curve values.

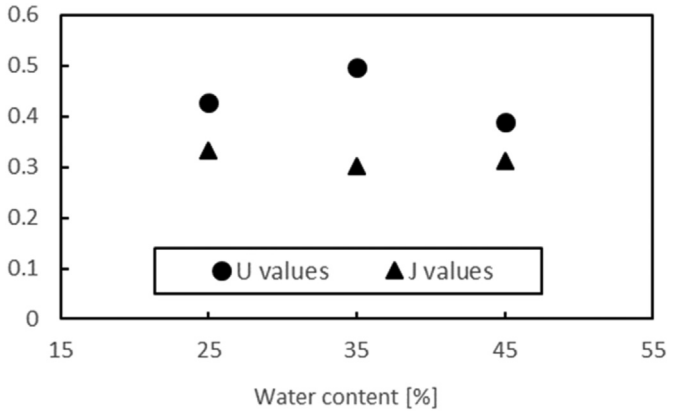

Fig. 9. Values of U and J for biochar produced at 600 °C and pelletized at 20 °C with different water contents.

large particles or chemical bonds and van der Waals's forces for small particles [35]. Water molecules can optimize the binding of particles by establishing bridges that connect the biomass particles when direct interactions among them do not exist [36]. As result of this, the use of water as binder is beneficial both as quality enhancer to improve the strength of pellets and as lubricant to smooth the process for pelletizing biomass particles. Considering the definitions of U and J in Eq. 3 and Eq. 4, it becomes plausible to assume that water acts on the three coefficients μ, P_{N0} and ν_{lr}. It could therefore be inferred that the pelleting process would benefit from a further increase in the water content to a certain extent. Instead, as observed in Ref. [37], an excess of water in the densification might cause particle-to-particle lubrication. As a result, the center of the pellet extrudes faster than the exterior and it is related to an increase of mechanical fragility. A similar behavior was also observed to affect biochar in some preliminary studies which were carried out for the preparation of the present work. However, biochar densification requires a considerable amount of water (or liquid binder, similar to water), since the solid bridges between particles are not enough to enhance plastic deformation. Without water or liquid binder, it would therefore become challenging to track the exiting pressure since the ejected material would still be in powder form. Therefore, the optimum content of binder to enhance a proper pelletization is expected to be within the range investigated in the present work. It also agrees with the results reported in Ref. [21].

3.3. Influence of pelleting temperature

Biochar produced at 600 °C was pelletized with a water content of 35% at different pelleting temperatures and the respective curves were derived. The results are shown in Fig. 10. The curves obtained with a pelleting temperature of 20 and 120 °C returned slightly higher exiting pressures in comparison with those obtained at 60 and 90 °C. The biochar produced at 600 °C has stable properties and is therefore not expected to change in the temperature range that was selected for these pelletization tests. The considerable amount of water as binder could instead affect the pelletization process in relation to the pelleting temperature, especially as the die temperature approaches 100 °C. However, no evident observations in this regard arise from the pelleting curves shown in Fig. 10. A possible reason might be the selected compression time, which was relatively short, in combination with the good homogeneity of the biochar-water mixture. Longer compression times might be useful to catch possible more evident differences between the pelleting curves.

Further observations can be drawn when the coefficients U and J are analyzed, as shown in Fig. 11. In Refs. [26,27], a decreasing trend for the coefficient U values was observed, while J was roughly constant, i.e. not influenced by the pelleting temperature. Similar trends are confirmed for the pelletization of biochar when varying pelleting temperature. The linear correlation of U presents a R^2 of 0.94, while it is easily visible that J oscillates around 0.30, with a maximum variation of 13%.

Such behavior makes it difficult to clearly define the dependence of pelleting temperature on the coefficients μ, P_{N0} and ν_{lr},

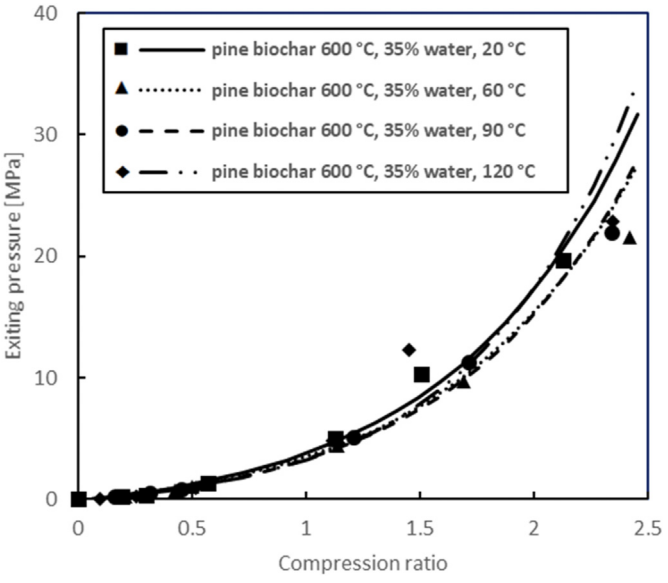

Fig. 10. Exiting pressure curves for biochar produced at 600 °C and pelletized at several temperatures with a water content of 35%. For each configuration, the legend shows a marker and a line. The markers display the experimental data, while the three line represents the modeled curve values.

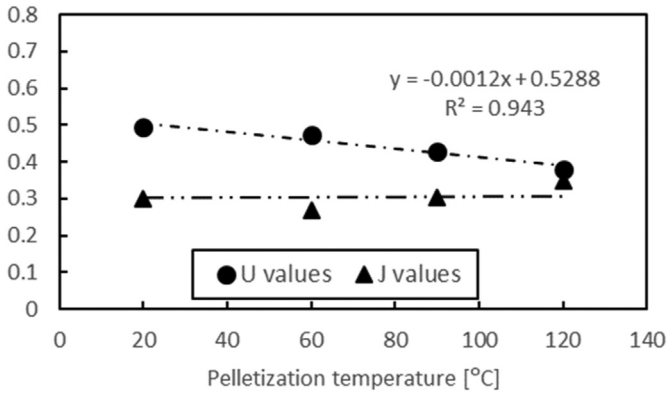

Fig. 11. Values of U and J for biochar produced at 600 °C and pelletized at increasing temperatures with a water content of 35%.

because they mutually affect the coefficients of the model. However, it is possible to simplify the model by assuming that U is linear and dependent on the temperature and that J is constant [26]. In this case, the average of the J values previously obtained and presented in Fig. 11 was selected as constant. With these assumptions, further attempts were made to analyze the effects of the pelleting temperature. The new pelletization exiting pressure curves are presented in Fig. 12. With the exception of some data points in the curves at 20 and 120 °C, the curves seem to fit successfully the experimental results. From the new simplified curves, it can be seen that the exiting pressure at fixed compression ratio decreases upon increasing the pelleting temperature. This agrees with what was observed in Refs. [20,21], where the cause was attributed to the plastic deformation of lignin as temperature above the glass transition temperature. However, by a certain extent, the content of lignin in the feedstock might be quite low and, hence, not enough to deform and behave as plastic and act as a binder as well. For such circumstances, water might be a principal driver which affects the pelletization process. At high pelletization temperatures, the water might evaporate and be present between the pellet and the die, acting as a lubricating layer which reduces the friction. The possibility of computing U by linear interpolation and setting J constant can nevertheless be assumed to provide acceptable accurate results to briefly evaluate the pelleting conditions by varying the process temperature, simplifying the operational analysis. Further investigations are needed to obtain better understanding of the effect of the temperature on the pelletization of biochar when using water as binder.

3.4. Influence of biochar production temperature

When the pelleting curves of biochar produced at different pyrolysis temperatures are compared, two clear trends are distinguishable. The curves are presented in Fig. 13 and the coefficients in Fig. 14. Compared to those pyrolyzed at 600 and 800 °C, biochar produced at 400 °C is characterized by a short linear region and a rapid exponential region, suggesting that the material might face practical challenges if compressed at industrial compression ratios (ca. 7–8). On the other hand, pelletization of biochar produced at 800 °C seems to perform better, and the exiting pressures are lower than that of the base case. When the coefficients U and J are analyzed in Fig. 13, it can be noticed that J reduces dramatically between 400 and 600 °C, while no evident trends are observable for U. It is hence not possible to reveal the reason for this behavior by only analyzing the coefficients. The benefit of pyrolyzing at higher temperatures are reported in similar works, where the focus was on the effects on mechanical properties of biochar pellets [18,20]. Therefore, it appears interesting to look further into this effect.

As explained in Ref. [38], higher pyrolysis temperatures result in a biochar structure with much less fibers but more brittle structure. For a specific grinding time, a larger fraction of small particles can therefore be obtained from the biochar sample produced at a higher pyrolysis temperature. The particle size distributions for biochar produced at 600 and 800 °C, as presented in Fig. 15, are

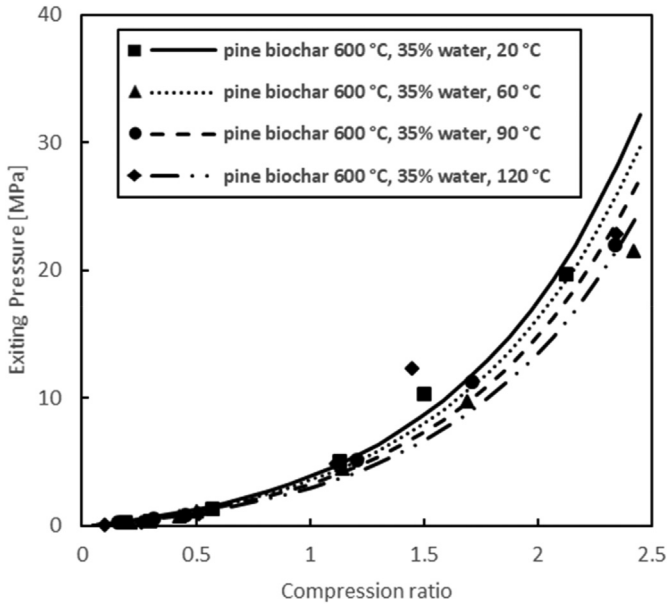

Fig. 12. Exiting pressure curves for biochar produced at 600 °C and pelletized at several temperatures with a water content of 35%, assuming U function of the pelleting temperature and J constant (0.30). For each configuration, the legend shows a marker and a line. The markers display the experimental data, while the three line represents the modeled curve values.

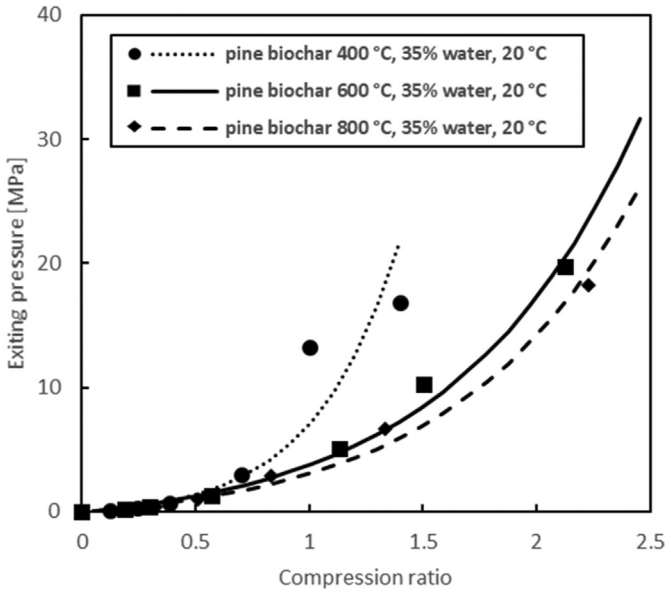

Fig. 13. Exiting pressure curves for biochar produced at different pyrolysis temperatures and pelletized at 20 °C with a water content of 35%. For each configuration, the legend shows a marker and a line. The markers display the experimental data, while the three line represents the modeled curve values.

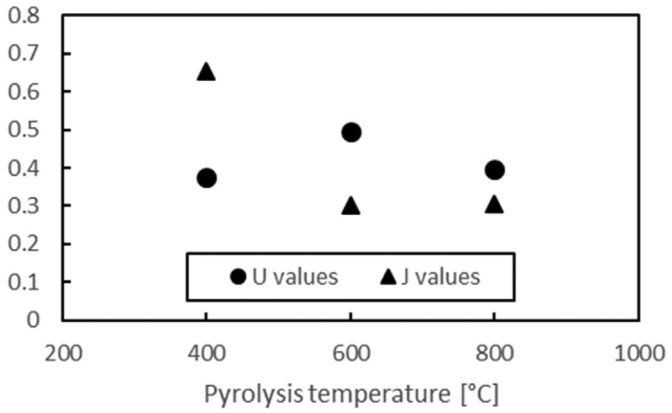

Fig. 14. Values of U and J for biochar produced at different pyrolysis temperatures and pelletized at 20 °C with a water content of 35%.

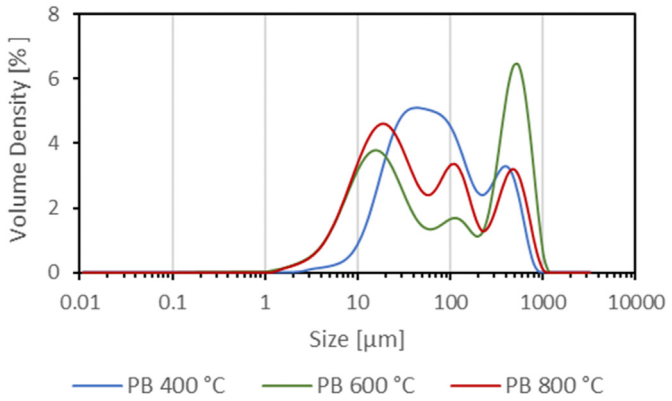

Fig. 15. Particle size distribution for pine biochar (PB) produced at 400, 600 and 800 °C.

similar and characterized by a wider range with a considerable peak at smaller particle sizes. In comparison, biochar produced at 400 °C has a narrower particle size distribution, and a significant fraction of the particles has larger particle sizes in the range of 50–100 μm. Due to the presence of smaller particles and wider particle size distribution, biochar pyrolyzed at higher temperature is expected to perform better in pelletization.

The biochar particles with different sizes have also a different capacity to adsorb and capture water. Therefore, as water is added as binder, the biochar particles with different sizes play different roles and affect the pelletization process. According to Ref. [39], porosity and hydrophobicity are the main biochar characteristics influencing the water uptake capacity of biochar. Pores can be divided in different classes according to their size. In biochar, they are mainly macropores (0.1–1000 μm) inherited by the woody structure and are not much affected by the pyrolysis process [40]. However, it was demonstrated that porosity increases considerably at higher pyrolysis temperatures due to the formation of micropores (0.0001–0.001 μm) [41], in agreement with the specific surface area and porosity analysis of the tested biochar shown in Table 2. Both surface areas and porosity are lowest for the biochar produced at 400 °C, while the biochars produced at 600 and 800 °C have significantly higher surface areas and porosity. A similar increase of surface area and porosity of biochar produced at higher temperatures are reported in Refs. [41,42]. The phenomenon is expected to be associated to the further devolatilization and carbonization of biomass, which occur at elevated pyrolysis

Table 2
Ultimate analysis, proximate analysis, BET and porosity of biochar produced at 400, 600 and 800 °C. The acronym db and wb stand for dry and wet basis. Standard deviations of proximate analysis results are included in parenthesis.

Pyrolysis temperature [°C]	400	600	800
Ultimate analysis			
C [% db]	74.1	85	94.3
H [% db]	4.4	2.6	1.3
N [% db]	–	–	–
O [% db]	21.5	12.4	4.4
Proximate analysis			
Fixed Carbon [% wb]	63.7 (±1.2)	85.2 (±0.5)	93.2 (±0.4)
Volatile matters [% wb]	34.2 (±0.6)	13.0 (±0.1)	4.3 (±0.3)
Ash [% wb]	1.3 (±0.1)	1.5 (±0.1)	1.5 (±0.1)
Moisture content [% wb]	0.8 (±1.0)	0.3 (±0.3)	1.0 (±0.3)
BET [m^2/g]	1.8	169.2	317.1
Porosity [cm^3/g]	0.003	0.115	0.140

temperatures [43]. This is confirmed by the considerably lower amount of oxygen obtained from the ultimate analysis and volatile matter from the proximate analysis (Table 2) for the samples produced at high temperatures. On the other hand, hydrophobicity of one material is heavily related to presence of the functional aliphatic group on the surface of the carbonaceous structure [44]. It has been stated that biochar pyrolyzed at temperatures higher than 600 °C generally lose this group [45]. Therefore, the surface of biochar produced at high temperatures will be more hydrophilic and more porous. Water can then be expected to penetrate more easily into the solid structure and the binding of particles will be enhanced. After the considerations discussed in Ref. [46], the hydrophobicity distinguishing biochar pyrolyzed at low temperatures might be overcome by introducing hydrophilic binders, e.g. lignin. However, hydrophobicity is also a desired property in the final pellets and the included binders might affect it, with consequences during the storing and handling [47]. It is important to mention that the relationship between pyrolysis temperature and hydrologic properties of biochar has been observed in a broad variety of both woody and non-woody pyrolyzed biomass [48]. As consequence, there is important evidence that pyrolysis temperature affects the performance of biochar in the pelleting phase and, if water is included as single binder, high pyrolysis temperature may improve the quality of the final pellets.

3.5. Influence of pyrolysis oil as binder

Pelletization of biochar with pyrolysis oil as binder were also studied and the pelleting curve is presented in Fig. 16. The oil produced during pyrolysis and then stored was used. 35% of pyrolysis oil was mixed with biochar produced at 600 °C for producing pellets, which was compared to the base case, as the 35% of water content was added with the same biochar. As shown in Fig. 16, no significant difference is visible between the curves obtained from tests using the two binders; however, pyrolysis oil returns somewhat lower values of exiting pressure. The pyrolysis oil used in the current work has a considerable water content (85.1 ± 1.4 wb%) and also contains a certain fraction of non-water compounds. According to Ref. [49], pyrolysis oil, produced at temperature between 600 and 900 °C, is characterized by high carbon content, but also a considerable oxygen content. In particular, at circa 600 °C, the main compounds are (in order of decreasing quantity): 1-hydroxy-2-butanone, hydroxyacetone, methanol and acetic acid [50]. How and in what extent these non-water compounds affect the pelletization and the pellets quality is however not clear. However, some of these compounds might affect the hygroscopic property of biochar, making it more hydrophilic

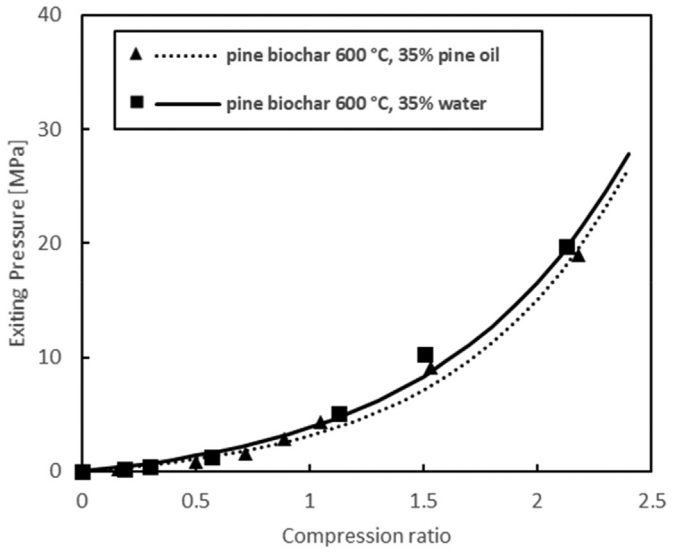

Fig. 16. Comparison between pelleting pressure curves of biochar produced at 600 °C and densified at 20 °C with either 35% of water content or of pyrolysis oil of total feedstock weight. For each configuration, the legend shows a marker and a line. The markers display the experimental data, while the three line represents the modeled curve values.

and, therefore, ease the binding with the water which is present with the pyrolysis oil. Considering the outstanding features associated to the use of pyrolysis oil as binder [20], it could be relevant to investigate which of these compounds has a major role in the enhancement of the binding mechanism, or what is the role of the carbon and oxygen content. In this way, the qualities of this binder could be further developed and upgraded. However, such research was beyond the scope of this work.

Fig. 17 shows representative SEM images of the morphology and microstructure of pellets from pine biochar produced at 800 °C with addition of 35% water (referred to as PB 800) and pine biochar produced at 600 °C with addition of 35% of pyrolysis oil (referred to as PB 600-O). These two configurations were compared because of their similar morphology. The comparison might therefore be helpful in identifying differences between the water and pyrolysis oil as binder. Both biochar pellets display compact and dense structure. Compared to PB 600-O, the PB 800 pellet has more smoothed surface. However, a few cracks highlighted by white arrows can be seen in Fig. 17 (a), which were not observed from the PB 600-O pellet in Fig. 17 (d). Presence of these cracks indicates more susceptible breakage of PB 800 during durability tests and further handling, transportation and storage. Fig. 17 (c) and (f) show images of areas highlighted respectively in Fig. 17 (b) and (e), with the same high magnification. Fig. 17 (c) shows that the biochar particles have rather smaller sizes, in comparison to the PB 600-O biochar pellet displayed in Fig. 17 (f). This is in line with particle size distribution analysis results shown in Fig. 15, where biochar produced at 600 °C has a larger fraction of particles with size in the range of 500–1000 μm.

3.6. Comparison with untreated wood and torrefied wood

The base case of this work was compared to pelleting curves of two different pine-based pellets: untreated wood (with a water content of 10%) and torrefied wood with a heating rate of 2 °C/min up to 275 °C for 2 h in nitrogen atmosphere (with a water content of 5%), processed and pelletized according to the methods used for the base case. The results are presented in Fig. 18. At high compression ratios, untreated pine was characterized by the lowest exiting pressures. The values were coherent with what was previously presented in Ref. [51]. When the exiting pressures in relation to the compression ratios are compared to several other feedstocks pelletized in Refs. [52,53], pine pellets return similar values, confirming that untreated softwood has favorable properties for the

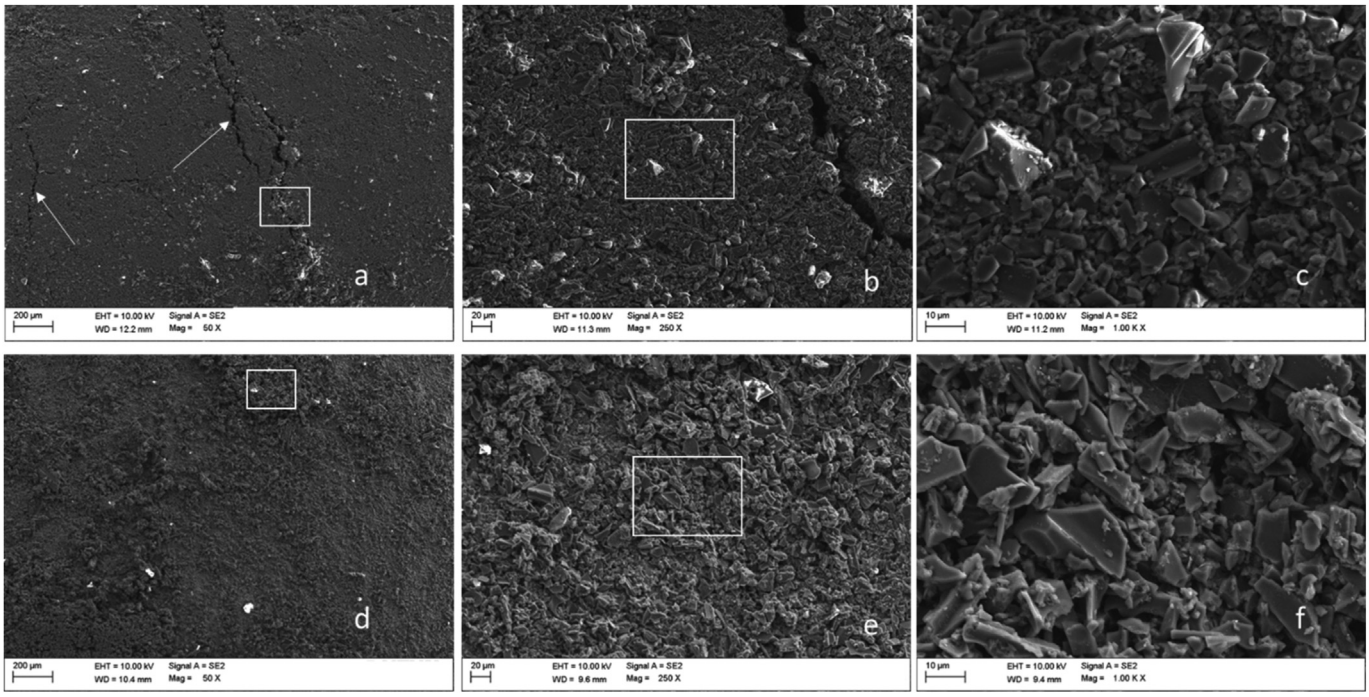

Fig. 17. SEM images of pine biochar produced at 800 °C ((a), (b) and (c)) with addition of 35% water and pine biochar produced at 600 °C with addition of 35% bio-oil ((d), (e) and (f)).

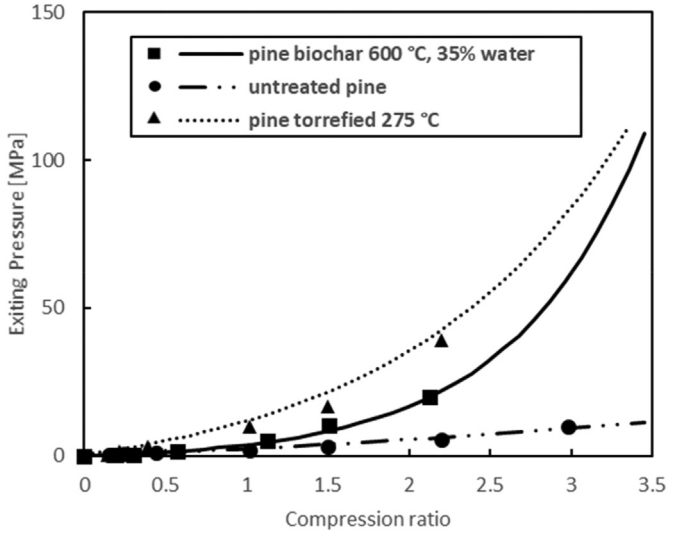

Fig. 18. Comparison between pelleting pressure curves of biochar produced at 600 °C and densified at 20 °C with a 35% water content, untreated pine woodchips pellets (water content 10%), woodchips torrefied at 275 °C (water content 5%) densified at 20 °C. For each configuration, the legend shows a marker and a line. The markers display the experimental data, while the three line represents the modeled curve values.

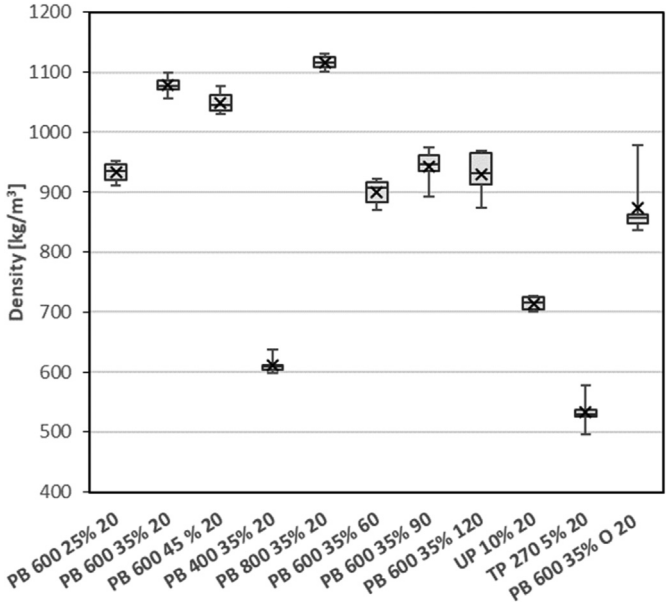

Fig. 19. Particle density of pellets studied and compared in this work. In the name code PB refers to pine biochar, UP to untreated pine, TP to torrefied pine. The first number following the type of treatment is the pyrolysis temperature in °C, then the percentage of water is signed and finally the pelleting temperature in °C. In the last label O stands for Oil, meaning the binder was pyrolysis oil.

pelletization. Due to similarities, it is worthy to compare the torrefied and pyrolyzed pine wood in terms of pelletization. Compared to torrefied wood, lower exiting pressures were obtained during pelletization of biochar produced at 600 °C. It is important to mention that the torrefaction settings were chosen as representative, without any concern about an optimal pelletization outcome. Moreover, as mentioned in Ref. [54], pelletization of torrefied wood requires higher temperatures to overcome the glass temperature of the lignin and enhance its binding properties. The pelleting curve obtained in this paper is comparable with published results [27,31]. At low compression ratios, torrefied pellets have higher exiting pressure values, indicating that the coefficient U is higher, as well. Therefore, according to Eq. 3, the torrefied material might be characterized by higher sliding friction coefficient and prestressing pressure. As mentioned in Ref. [26], these terms are complex to compute and hardly obtainable in literature. However, it is possible to attempt an explanation focusing on the different degrees of carbonization and thermal degradation generated by pyrolysis and torrefaction. While hemicellulose mainly degrades in temperature ranges between 250 and 300 °C, followed by extensive cellulose degradation at slightly higher temperatures (275–350 °C [55]), lignin degradation occurs in a much wider temperature range, up to above 600 °C [56]. Hence, torrefied wood at 270 °C contains still a relevant amount of hemicellulose and most of the cellulose [36], which will play a considerable positive role during the pelletization process. In contrast, the three main components in biomass are almost completely degraded after the pyrolysis treatment and following carbonization [57]. In addition, biochar has graphene-like sheets structure, causing an increase of the elasticity of the material [58]. This behavior might therefore be associated to a decrease of the prestressing term, impacting on the coefficient U. This could explain the different trend in the linear region for torrefied and pyrolyzed pellets.

3.7. Influence on mechanical properties

For each configuration tested in this work, the density and the compressive strength of the pellets were measured, after the considerations risen from Fig. 6. The results are presented in Fig. 19 and Fig. 20. In Fig. 19 the density of produced biochar pellets is compared. The pellets from biochar produced at 800 °C had the highest density, followed by the ones from biochar produced at 600 °C and at 400 °C. The effect of the pyrolysis temperature on the biochar pellet density appears to align with the analysis of pelleting curves: the lower the values of exiting pressure at fixed compression ratio, the higher the density of the produced biochar pellet. The results indicate that a smooth pelleting process yielding dense pellets is feasible and also easier to manage and work with. This is however not enough to justify a general strong correlation between pelleting pressure and density since untreated wood pellets presented contrasting results. It could therefore be inferred that the properties of the pelletized material can also considerably affect the characteristics of pellets, to a higher extent than the pelleting process. However, in this case, it is noteworthy to mention that the wood pellets were characterized by lower density values than what are generally observed, since the pelleting temperature was not high enough to enhance the lignin binding mechanism [59]. Quite interestingly, when varying the water content, the maximum density of biochar pellets was observed at the value of 35%, while it was slightly lower with 45% of water content. Since the water is denser than biochar, an increase of binder content might easily be related to an increase of density. The results suggest that above a certain threshold the porous structure of biochar cannot absorb all the water and gets over-saturated. Density was negatively affected by an increase in pelleting temperature. The increase of temperature enhances water evaporation during the process and give negative effects on densification of biochar. Indeed, at higher pelleting temperatures, the density value is similar to the one observed for pellets with 25% of water content, demonstrating that a relevant amount of water was lost. When pyrolysis oil was used as binder, the density of biochar pellet was lower and characterized by a considerably high uncertainty. Pyrolysis oil is tendentially unstable and a relevant amount was presumably volatized in the

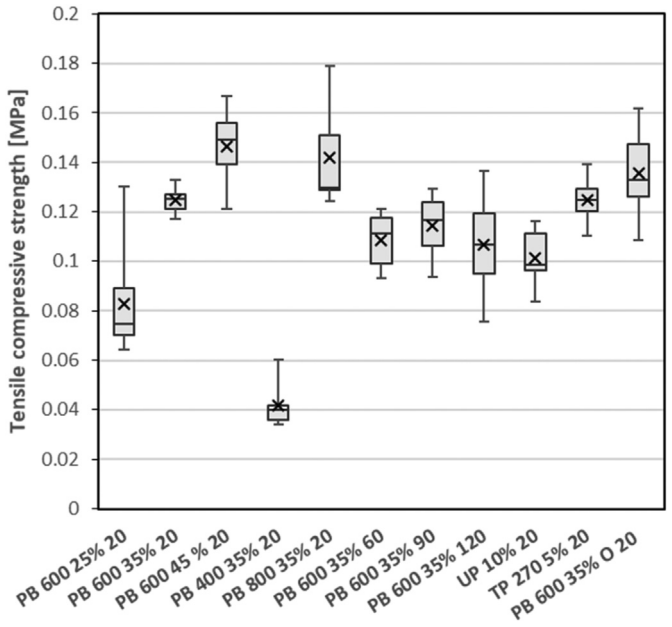

Fig. 20. Tensile compressive strength of pellets studied and compared in this work. In the name code PB refers to pine biochar, UP to untreated pine, TP to torrefied pine. The first number following the type of treatment is the pyrolysis temperature in Celsius degrees, then the percentage of water is signed and finally the pelleting temperature in degrees Celsius. In the last label O stands for Oil, meaning the binder was pyrolysis oil.

pellets cooling phase, with a consequent decrease in density.

Fig. 20 reports the value of the tensile compressive strength of produced biochar pellets. The positive effect of an increase of pyrolysis temperature was confirmed, suggesting a possible correlation between density and strength, too. In this case, pellets with biochar produced at 600 and 800 °C have similar strength values. This result, combined with the analysis of the modeled curves and density values, suggests that it is not necessary to carry out pyrolysis at excessively high temperatures to obtain a sufficient mechanical pellet quality and contain the energy consumption in the pelleting process. Compressive strength seems to benefit of an increased water content. This result, combined with the water content effects on density presented in Fig. 19, confirms that generally low moisture content is associated to mechanical weakness of biochar pellets, while too high moisture content affects negatively density [34]. Nevertheless, as explained in Ref. [60] for biomass in general, and verified in Refs. [20,21] for biochar, an excessive moisture content might lead to incompressibility and hence mechanically weaker pellets. This behavior is strictly close to what is observed for density, confirming that the binding mechanism between biochar and water are partially compromised. These results show that, as a rule of thumb, the trend in the modeled pelleting curves can already give important information about the mechanical properties of the pellets. However, no statistically significant correlations could be derived. Different than density, strength of produced biochar pellets is higher when water is substituted by pyrolysis oil. Despite the water volatilization affecting the density of the pellets, the composition of the pyrolysis oil provides a stronger binding mechanism, making it a promising binder. In conclusion, based on the results illustrated in Figs. 19 and 20, it is reasonable to assume that, among the factors investigated in the present work, pyrolysis temperature is the most critical factor to both optimize the pelleting process and obtain mechanical properties comparable to industrially established pelletized materials. Moreover, the results confirm the potential of using pyrolysis oil as a binder in alternative to water.

4. Conclusions

This work intended to enlighten on the mechanism underneath the pelleting process of pyrolyzed biomass by the help of a multiparameter model previously implemented and used to analyze pelletization of wood and torrefied wood. The preliminary evaluation of biochar pelleting behavior based on lab scale analysis can facilitate the feasibility evaluation of industrial biochar densification processes, which recently has turned to be promising for cofiring and metallurgical applications. The multiparameter model was firstly applied to a base case (pine pyrolyzed at 600 °C mixed with 35% of water and pelletized at 20 °C) and the feasibility of fitting the pelleting pressure as function of the compression ratio was verified. Afterwards, starting from pine, pelleting curves modeling the variation of the exiting pressure in relation to the compression ratio of the pellets were built, with variation of water content (between 25 and 45%), pelleting temperature (between 20 and 120 °C), and pyrolysis temperature (between 400 and 800 °C). For biochar pellets produced under each configuration, density and tensile compressive strength were measured to analyze the mechanical quality of the pellets. It was hence found out that:

- Pelletization of biochar requires lower exiting pressures with increasing water contents. Compressive strength benefits also from higher water contents, while the density gets reduced at high water content.
- The pelleting temperature did not particularly affect the exiting pellet pressure, while both density and compressive strength are tendentially higher at lower pelleting temperatures. It can therefore be stated that during pelletization, effects of other parameters should be considered more carefully than the pelleting temperature. Among the different cases, the pelleting curves at different pelleting temperatures were the only ones characterized by a linear trend for the coefficient U. When computing J by assuming linearity of J, the curves were still close to the empirical data, suggesting that this parameter is hence the easiest to model.
- The model for different pyrolysis temperatures returned the curves most deviating from each other. In particular, a considerable influence on pelleting pressure was observed between biochar produced at 400 and 600 °C. Especially for biochar produced at 400 °C, the outcome showed that pelletization of such material would be challenging. On the other hand, no relevant differences were noticed between 600 and 800 °C. The same trend was observed for density and compressive strength. Such result suggests that, it is necessary to pyrolyze at relatively high temperatures to facilitate densification,

Water was compared with pyrolysis oil to evaluate its performance as binder in the pelleting phase. The same percentage 35% wt water and pyrolysis oil was considered and tested as binder, respectively. The comparison between pellet exiting pressures for water and pyrolysis oil as binder did not provide relevant differences. Moreover, when the mechanical properties were measured, it was observed that a reduction in density is balanced by an increase in compressive strength.

Finally, the base case was compared to the pelleting curves of untreated pine and torrefied pine. Tests were carried out to understand both the feasibility of biochar pelletization in relation to more established pelleting technology and in what extent they differ. Wood pellets proved to be easier to pelletize, however, biochar pellets showed exiting pressure values lower than for torrefied pellets.

Results from the current work contribute to better understandings on biochar densification, offering an exhaustive

insight useful to comprehend some basic phenomena which might occur in the pelleting process and easing further and more detailed studies.

Credit author statement

Lorenzo Riva: Conceptualization, Methodology, Experiments Validation, Investigation, Data curation, Writing – review & editing, Liang Wang: Experiments, Investigation, Data curation, Writing – review & editing, Giulia Ravenni: Experiments, Conceptualization, Methodology, Review & Editing, Pietro Bartocci: Data curation, Supervision, Review, Resources, Therese V. Buø: Supervision: Conceptualization, Resources, Supervision, Øyvind Skreiberg: Writing, Supervision, Review & Editing, Francesco Fantozzi: Supervision, Resources, Henrik Kofoed Nielsen: Supervision, Resources, Writing – review & editing

Declaration of competing interest

The authors declare that they have no known competing financial interests or personal relationships that could have appeared to influence the work reported in this paper.

Acknowledgments

SINTEF Energy Research acknowledges the financial support from the Research Council of Norway and a number of industrial partners through the project BioCarbUp ("Optimising the biocarbon value chain for sustainable metallurgical industry", grant number 294679/E20).

References

[1] Huang Y-F, Syu F-S, Chiueh P-T, Lo S-L. Life cycle assessment of biochar cofiring with coal. Bioresour Technol Mar. 2013;131:166–71. https://doi.org/10.1016/j.biortech.2012.12.123.
[2] Huang C-W, Li Y-H, Xiao K-L, Lasek J. Cofiring characteristics of coal blended with torrefied Miscanthus biochar optimized with three Taguchi indexes. Energy Apr. 2019;172:566–79. https://doi.org/10.1016/j.energy.2019.01.168.
[3] Wang L, Várhegyi G, Skreiberg Ø. CO_2 gasification of torrefied wood: a kinetic study. Energy Fuels Dec. 2014;28(12):7582–90. https://doi.org/10.1021/ef502308e.
[4] Wang L, Várhegyi G, Skreiberg Ø, Li T, Grønli M, Antal MJ. Combustion characteristics of biomass charcoals produced at different carbonization conditions: a kinetic study. Energy Fuels Apr. 2016;30(4):3186–97. https://doi.org/10.1021/acs.energyfuels.6b00354.
[5] Agirre I, Griessacher T, Rösler G, Antrekowitsch J. Production of charcoal as an alternative reducing agent from agricultural residues using a semi-continuous semi-pilot scale pyrolysis screw reactor. Fuel Process Technol Feb. 2013;106:114–21. https://doi.org/10.1016/j.fuproc.2012.07.010.
[6] Dufourny A, Van De Steene L, Humbert G, Guibal D, Martin L, Blin J. Influence of pyrolysis conditions and the nature of the wood on the quality of charcoal as a reducing agent. J Anal Appl Pyrol Jan. 2019;137:1–13. https://doi.org/10.1016/j.jaap.2018.10.013.
[7] Griessacher T, Antrekowitsch J, Steinlechner S. Charcoal from agricultural residues as alternative reducing agent in metal recycling. Biomass Bioenergy 2012;39:139–46. https://doi.org/10.1016/j.biombioe.2011.12.043.
[8] El-Naggar A, et al. Biochar composition-dependent impacts on soil nutrient release, carbon mineralization, and potential environmental risk: a review. J Environ Manag Jul. 2019;241:458–67. https://doi.org/10.1016/j.jenvman.2019.02.044.
[9] Purakayastha TJ, et al. A review on biochar modulated soil condition improvements and nutrient dynamics concerning crop yields: pathways to climate change mitigation and global food security. Chemosphere Jul. 2019;227:345–65. https://doi.org/10.1016/j.chemosphere.2019.03.170.
[10] Zhang G, Guo X, Zhu Y, Han Z, He Q, Zhang F. Effect of biochar on the presence of nutrients and ryegrass growth in the soil from an abandoned indigenous coking site: the potential role of biochar in the revegetation of contaminated site. Sci Total Environ Dec. 2017;601–602:469–77. https://doi.org/10.1016/j.scitotenv.2017.05.218.
[11] Luo L, et al. The characterization of biochars derived from rice straw and swine manure, and their potential and risk in N and P removal from water. J Environ Manag Sep. 2019;245:1–7. https://doi.org/10.1016/j.jenvman.2019.05.072.
[12] Perez-Mercado LF, Lalander C, Joel A, Ottoson J, Dalahmeh S, Vinneråas B. Biochar filters as an on-farm treatment to reduce pathogens when irrigating with wastewater-polluted sources. J Environ Manag Oct. 2019;248:109295. https://doi.org/10.1016/j.jenvman.2019.109295.
[13] Intergovernmental Panel on climate change, "Global Warming of 1.5°C. 2019.
[14] Wang J, Wang S. Preparation, modification and environmental application of biochar: a review. J Clean Prod Aug. 2019;227:1002–22. https://doi.org/10.1016/j.jclepro.2019.04.282.
[15] Zhang Z, Zhu Z, Shen B, Liu L. Insights into biochar and hydrochar production and applications: a review. Energy Mar. 2019;171:581–98. https://doi.org/10.1016/j.energy.2019.01.035.
[16] Sun X, Li M, Chen Y. Biochar facilitated bioprocessing and biorefinery for productions of biofuel and chemicals: a review. *Bioresource Technology*; Oct. 2019. p. 122252. https://doi.org/10.1016/j.biortech.2019.122252.
[17] Wang L, Buvarp F, Skreiberg Ø, Bartocci P. A study on densification and CO2 gasification of biocarbon. In *chemical engineering transactions*, vol. 65; 2018. p. 145–50. Bologna, Italy.
[18] Hu Q, et al. The densification of bio-char: effect of pyrolysis temperature on the qualities of pellets. Bioresour Technol 2016;200:521–7. https://doi.org/10.1016/j.biortech.2015.10.077.
[19] Kang K, et al. Codensification of Eucommia ulmoides Oliver stem with pyrolysis oil and char for solid biofuel: an optimization and characterization study. Appl Energy 2018;223:347–57. https://doi.org/10.1016/j.apenergy.2018.04.069.
[20] Riva L, Surup GR, Buø TV, Nielsen HK. A study of densified biochar as carbon source in the silicon and ferrosilicon production. Energy Aug. 2019;181:985–96. https://doi.org/10.1016/j.energy.2019.06.013.
[21] Riva L, et al. Analysis of optimal temperature, pressure and binder quantity for the production of biocarbon pellet to be used as a substitute for coke. Appl Energy 2019;256:113933. https://doi.org/10.1016/j.apenergy.2019.113933.
[22] Bartocci P, et al. Biocarbon pellet production: optimization of pelletizing process. Chemical engineering transactions, vol. 65; 2018. p. 355–60. https://doi.org/10.3303/CET1865060. Bologna, Italy.
[23] Bazargan A, Rough SL, McKay G. Compaction of palm kernel shell biochars for application as solid fuel. Biomass Bioenergy 2014;70:489–97. https://doi.org/10.1016/j.biombioe.2014.08.015.
[24] Holm JK, Henriksen UB, Hustad JE, Sørensen LH. Toward an understanding of controlling parameters in softwood and hardwood pellets production. Energy Fuels Nov. 2006;20(6):2686–94. https://doi.org/10.1021/ef0503360.
[25] Holm JK, Henriksen UB, Wand K, Hustad JE, Posselt D. Experimental verification of novel pellet model using a single pelleter unit. Energy Fuels Jul. 2007;21(4):2446–9. https://doi.org/10.1021/ef070156l.
[26] Holm JK, Stelte W, Posselt D, Ahrenfeldt J, Henriksen UB. Optimization of a multiparameter model for biomass pelletization to investigate temperature dependence and to facilitate fast testing of pelletization behavior. Energy Fuels Aug. 2011;25(8):3706–11. https://doi.org/10.1021/ef2005628.
[27] Puig-Arnavat M, Ahrenfeldt J, Henriksen UB. Validation of a multiparameter model to investigate torrefied biomass pelletization behavior. Energy Fuels Feb. 2017;31(2):1644–9. https://doi.org/10.1021/acs.energyfuels.6b02895.
[28] Lestander TA, Rudolfsson M, Pommer L, Nordin A. NIR provides excellent predictions of properties of biocoal from torrefaction and pyrolysis of biomass. Green Chem 2014;16(12):4906–13. https://doi.org/10.1039/C3GC42479K.
[29] Reza MT, Uddin MH, Lynam JG, Coronella CJ. Engineered pellets from dry torrefied and HTC biochar blends. Biomass Bioenergy Apr. 2014;63:229–38. https://doi.org/10.1016/j.biombioe.2014.01.038.
[30] L, Wang L, Riva Ø, Skreiberg R, Khalil P, Bartocci Q, Yang H, Yang X, Wang D, Chen M, Rudolfsson HK. Nielsen, effect of torrefaction on properties of pellets produced from woody biomass energy and fuels. 2020. https://doi.org/10.1021/acs.energyfuels.0c02671.
[31] Y, Zhang F, Chen D, Chen K, Cen J, Zhang X, Cao. Upgrading of biomass pellets by torrefaction and its influence on the hydrophobicity, mechanical property, and fuel quality. Biomass Conversion and Biorefinery; 2020. https://doi.org/10.1007/s13399-020-00666-5.
[32] Shaw MD, Karunakaran C, Tabil LG. Physicochemical characteristics of densified untreated and steam exploded poplar wood and wheat straw grinds. Biosyst Eng 2009;103(2):198–207. https://doi.org/10.1016/j.biosystemseng.2009.02.012.
[33] Shang L, et al. "Lab and bench-scale pelletization of torrefied wood chips—-process optimization and pellet quality. Bioenerg. Res. Mar. 2014;7(1):87–94. https://doi.org/10.1007/s12155-013-9354-z.
[34] Samuelsson R, Larsson SH, Thyrel M, Lestander TA. Moisture content and storage time influence the binding mechanisms in biofuel wood pellets. Appl Energy Nov. 2012;99:109–15. https://doi.org/10.1016/j.apenergy.2012.05.004.
[35] Nielsen SK, Rezaei H, Mandø M, Sokhansanj S. Constitutive modelling of compression and stress relaxation in pine pellets. Biomass Bioenergy Nov. 2019;130:105370. https://doi.org/10.1016/j.biombioe.2019.105370.
[36] Larsson SH, Rudolfsson M, Nordwaeger M, Olofsson I, Samuelsson R. Effects of moisture content, torrefaction temperature, and die temperature in pilot scale pelletizing of torrefied Norway spruce. Appl Energy Feb. 2013;102:827–32. https://doi.org/10.1016/j.apenergy.2012.08.046.
[37] Kaliyan N, Vance Morey R. Factors affecting strength and durability of densified biomass products. Biomass Bioenergy 2009;33(3):337–59. https://doi.org/10.1016/j.biombioe.2008.08.005.
[38] Wang L, et al. Impact of torrefaction on woody biomass properties. Energy

Procedia May 2017;105:1149–54. https://doi.org/10.1016/j.egypro.2017.03.486.
[39] Suliman W, Harsh JB, Abu-Lail NI, Fortuna A-M, Dallmeyer I, Garcia-Pérez M. The role of biochar porosity and surface functionality in augmenting hydrologic properties of a sandy soil. Sci Total Environ Jan. 2017;574:139–47. https://doi.org/10.1016/j.scitotenv.2016.09.025.
[40] Surup GR, Nielsen HK, Heidelmann M, Anna Trubetskaya. "Characterization and reactivity of charcoal from high temperature pyrolysis (800–1600 °C). Fuel Jan. 2019;235:1544–54. https://doi.org/10.1016/j.fuel.2018.08.092.
[41] Brewer CE, et al. New approaches to measuring biochar density and porosity. Biomass Bioenergy 2014;66:176–85. https://doi.org/10.1016/j.biombioe.2014.03.059.
[42] Jimenez-Cordero D, Heras F, Alonso-Morales N, Gilarranz MA, Rodriguez JJ. Porous structure and morphology of granular chars from flash and conventional pyrolysis of grape seeds. Biomass Bioenergy Jul. 2013;54:123–32. https://doi.org/10.1016/j.biombioe.2013.03.020.
[43] Antal MJ, Grønli M. The art, science, and technology of charcoal production. Ind Eng Chem Res 2003;42(8):1619–40. https://doi.org/10.1021/ie0207919.
[44] Das O, Sarmah AK. "The love–hate relationship of pyrolysis biochar and water: a perspective. Sci Total Environ 2015;512(513):682–5. https://doi.org/10.1016/j.scitotenv.2015.01.061.
[45] Gray M, Johnson MG, Dragila MI, Kleber M. Water uptake in biochars: the roles of porosity and hydrophobicity. Biomass Bioenergy 2014;61:196–205. https://doi.org/10.1016/j.biombioe.2013.12.010.
[46] Hu Q, Shao J, Yang H, Yao D, Wang X, Chen H. Effects of binders on the properties of bio-char pellets. Appl Energy 2015;157:508–16. https://doi.org/10.1016/j.apenergy.2015.05.019.
[47] Liu Z, Quek A, Kent Hoekman S, Balasubramanian R. Production of solid biochar fuel from waste biomass by hydrothermal carbonization. Fuel Jan. 2013;103:943–9. https://doi.org/10.1016/j.fuel.2012.07.069.
[48] Kinney TJ, et al. Hydrologic properties of biochars produced at different temperatures. Biomass Bioenergy Jun. 2012;41:34–43. https://doi.org/10.1016/j.biombioe.2012.01.033.
[49] Demirbas MF. Characterization of bio-oils from spruce wood (*Picea orientalis* L.) via pyrolysis. Energy Sources, Part A Recovery, Util Environ Eff Mar. 2010;32(10):909–16. https://doi.org/10.1080/15567030903059970.
[50] Demirbas A. The influence of temperature on the yields of compounds existing in bio-oils obtained from biomass samples via pyrolysis. Fuel Process Technol Jun. 2007;88(6):591–7. https://doi.org/10.1016/j.fuproc.2007.01.010.
[51] Lam PY, Lam PS, Sokhansanj S, Bi XT, Lim CJ, Melin S. Effects of pelletization conditions on breaking strength and dimensional stability of Douglas fir pellet. Fuel Jan. 2014;117:1085–92. https://doi.org/10.1016/j.fuel.2013.10.033.
[52] Stelte W, Clemons C, Holm JK, Ahrenfeldt J, Henriksen UB, Sanadi AR. Fuel pellets from wheat straw: the effect of lignin glass transition and surface waxes on pelletizing properties. Bioenerg. Res. Jun. 2012;5(2):450–8. https://doi.org/10.1007/s12155-011-9169-8.
[53] Puig-Arnavat M, Shang L, Sárossy Z, Ahrenfeldt J, Henriksen UB. "From a single pellet press to a bench scale pellet mill — pelletizing six different biomass feedstocks. Fuel Process Technol Feb. 2016;142:27–33. https://doi.org/10.1016/j.fuproc.2015.09.022.
[54] Stelte W, Sanadi AR, Shang L, Holm JK, Ahrenfeldt J, Henriksen UB. "Recent developments in biomass pelletization – a review. BioResources 2012;7(3):4451–90.
[55] Poletto M, Zattera AJ, Forte MMC, Santana RMC. Thermal decomposition of wood: influence of wood components and cellulose crystallite size. Bioresour Technol Apr. 2012;109:148–53. https://doi.org/10.1016/j.biortech.2011.11.122.
[56] Ren S, Lei H, Wang L, Bu Q, Chen S, Wu J. Thermal behaviour and kinetic study for woody biomass torrefaction and torrefied biomass pyrolysis by TGA. Biosyst Eng Dec. 2013;116(4):420–6. https://doi.org/10.1016/j.biosystemseng.2013.10.003.
[57] Bruun EW, et al. Influence of fast pyrolysis temperature on biochar labile fraction and short-term carbon loss in a loamy soil. Biomass Bioenergy Mar. 2011;35(3):1182–9. https://doi.org/10.1016/j.biombioe.2010.12.008.
[58] Barsoum MW, Murugaiah A, Kalidindi SR, Zhen T, Gogotsi Y. Kink bands, nonlinear elasticity and nanoindentations in graphite. Carbon 2004;42(8–9):1435–45. https://doi.org/10.1016/j.carbon.2003.12.090.
[59] Bergström D, et al. Effects of raw material particle size distribution on the characteristics of Scots pine sawdust fuel pellets. Fuel Process Technol Dec. 2008;89(12):1324–9. https://doi.org/10.1016/j.fuproc.2008.06.001.
[60] Kaliyan N, Morey RV. Natural binders and solid bridge type binding mechanisms in briquettes and pellets made from corn stover and switchgrass. Bioresour Technol Feb. 2010;101(3):1082–90. https://doi.org/10.1016/j.biortech.2009.08.064.